

In the author's opinion, significant increase in the laser propulsion efficiency can be attained by using energetic propellants of CHO-chemical composition, in which the laser pulse initiates chemical reactions with a noticeable chemical energy release. To find out the influence of energy characteristics of the CHO-materials upon the production efficiency of the laser propulsion, a number of polymeric and polycrystalline materials of CHO compositions with the negative oxygen balance [10] was studied including the specific heat of the combustion, the detonation, and the delayed burning of detonation products. It is known [11] that the laser radiation induces evaporation and the thermal decomposition of the CHO-materials. This is a pyrolysis starting at the temperature of 500–700 °C in the absence of oxygen. In air, the reaction of the high-temperature oxidation (combustion) of the pyrolysis products results in the energy release via two successive chemical reactions, namely, the detonation and the delayed burning of detonation products: $Q = Q_{\text{det}} + NQ_{\text{db}}$, where N is the coefficient of afterburning of detonation products. The energy of the detonation and delayed burning reactions may be calculated by the Hess law [11]:

$$Q_{\text{det}} = -(\Delta H_{\text{pr}} - \Delta H_{f298}^o); \quad Q_{\text{db}} = -\Delta H_{\text{pr}}$$

where ΔH_{pr} is the enthalpy of the reaction products; and ΔH_{f298}^o is the enthalpy of the material.

The energy balance of vapors of CHO-materials and the combustion of its components in oxygen of the air, which corresponds to standard conditions of laboratory experiments at the laser ablation of the materials, can be expressed in the following form:

$$(M + m) \frac{v^2}{2} = \beta[\alpha E + mQ]$$

where m is the mass of the evaporated material; M is the air mass in a volume of the laser propulsion nozzle; v is the average exhaust velocity; α is the coefficient of the laser energy conversion into heat energy of the propellant; and β is the coefficient of the conversion of propellant heat energy into the exhaust flow kinetic energy.

Then in accordance with the general definition of the momentum coupling coefficient C_m , one has:

$$C_{m1} = \frac{J}{E} = \frac{Mv}{E} = \sqrt{\frac{2M\beta\alpha}{E}};$$

$$C_{m2} = \frac{J}{E} = \frac{(M + m)v}{E} = \sqrt{\frac{2(M + m)\beta[\alpha E + mQ]}{E^2}}$$

where C_{m1} is the momentum coupling coefficient of the laser air-breathing propulsion under atmospheric conditions; C_{m2} is the momentum coupling coefficient with the CHO-materials as the auxiliary propellants. The relative increase

K (an efficient factor) of the momentum coupling coefficient can be defined in the case of the use of the laser detonation as

$$K = \frac{C_{m2}}{C_{m1}} = \sqrt{\left(1 + \frac{m}{M}\right) \left(1 + \frac{mQ}{\alpha E}\right)}.$$

To analyze the thrust impulse production in LPE with CHO-chemical solid propellants, the parameter of specific ablation energy $Q^* = E/m$ [8] can be used in addition. Then one consequently has:

$$K = \frac{C_{m2}}{C_{m1}} = \sqrt{\left(1 + \frac{m}{M}\right) \left(1 + \frac{Q}{\alpha Q^*}\right)}.$$

Figure 1 demonstrates the experimental results for C_m as a function of K $\sim [1 + 2.5(Q_{\text{det}}/Q^* + NQ_{\text{db}}/Q^*)]^{1/2}$ for polymeric propellants (1) over the range $1.75 \leq K \leq 3.12$ under atmospheric conditions without regard to the presence of oxygen in the polymer composition. Diagram 2 corresponds to the dependence of C_m upon K for polycrystalline propellants, the values of which for polyoxymethylene ($N = 1$), metaldehyde, and carbamoyl hydrazine ($N > 1$) are proportional over the range $3.08 \leq K \leq 5.96$. The values of C_m vs. K for dihydroxybenzene and oxybenzoic acid ($N < 1$) have a large spread and do not correspond to the dependence of C_m on K .

The experiments showed that the delayed burning of detonation products of the evaporated CHO-materials under the laser detonation in oxygen of the air is similar for all of the materials. And the reaction is the oxidation of the released atomic carbon and gaseous hydrogen with a formation of carbon dioxide and water molecules. At that, the delayed burning takes place sequentially to the detonation reaction and is limited by the bounded content of oxygen in the atmosphere air.

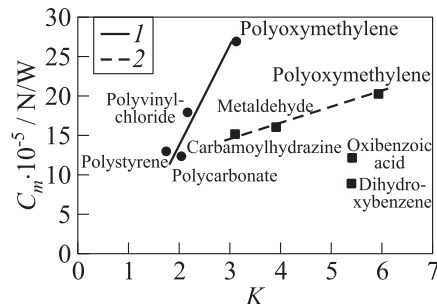


Figure 1 Dependence of C_m on K for polymeric (1) and polycrystalline (2) CHO-type propellants at atmosphere conditions [10]

Analysis of the experimental data on the laser propulsion with the polymeric materials used in the form of a plane target [10] shows that the maximal $C_m = 27 \cdot 10^{-5}$ N/W relates to polyoxymethylene, an oxygen-containing linear polymer with a high detonation component in the momentum coupling coefficient. The polymer has a pronounced region of the CO₂-laser radiation absorption by the C–O–C stretching vibrations.

The experiments show also that the efficient factor K can be applied to selecting of the polymer propellants for laser propulsion. For example, a moderate K is achieved for polymers with high Q^* (5,000–50,000 kJ/kg) that agrees well with the sufficiently high experimental values of C_m . In the case of the polycrystalline materials the values of Q^{**} are significantly lower (1200–4000 kJ/kg) that leads to a noticeable increase of K (two times for polyoxymethylene). But C_m for polycrystalline propellants is nevertheless 2.5 times less than the forecast increase. At that, for both polymeric and polycrystalline propellants their own proportional dependence of C_m upon K (for $N \geq 1$) is observed.

As one can see, the use of only laser ablation technique to produce a thrust does not allow to sufficiently increase the production efficiency by laser power. To reach a higher laser propulsion efficiency, the author suggests to use a combined mechanism of the thrust production when the laser ablation of solid (or liquid) propellants is realized inside a combustion chamber and special device is used to form an impulse as conventional jet engines produce.

In this case, the total efficiency of laser propulsion with energetic materials can be written as a relation of the power of an exhaust jet to the total power of heat sources in a combustion chamber of LPE in the following manner:

$$\eta_{\text{LPE}} = \frac{\beta(\alpha + mQ/E)}{1 + mQ/E}.$$

The results on η_{LPE} with Delrin® and polymethylmethacrylate (PMMA), studied in the experiments and re-calculated for space and atmosphere conditions, are listed in Table 1.

Atmosphere conditions of the thrust production mean the condition of delayed burning of the combustion products in the presence of the atmosphere

Table 1 Efficiency η_{LPE} of the experimentally tested CHO-materials ($\lambda = 10.6 \mu\text{m}$; $\alpha = 0.4$; and $\beta = 0.9$)

CHO-material	$E, \text{ J}$	$\dot{m}Q_{\text{det}}, \text{ J}$	$\dot{m}Q_{\text{det}}/E$	$\eta_{\text{LPE}},$ space/atmosphere conditions
Delrin® [10]	61.0	33.19	0.54	0.55/0.81
Delrin® [10]	57.1	21.60	0.38	0.51/0.78
PMMA [12]	90.0	18.51	0.21	0.45/0.86
PMMA [12]	130.0	19.73	0.15	0.43/0.85

oxygen. As one can see, a sufficient increase in the efficiency of laser propulsion is observed in the case when a complete propellant burning is achieved. To satisfy this condition, a space vehicle should imply both a CHO-propellant and auxiliary oxygen onboard. In accordance with the chemical reactions following the laser detonation of CHO-polymers, it will require about 1.067 kg (746.7 l) of oxygen for 1 kg of $(\text{CH}_2\text{O})_n$.

3 TECHNICAL FEATURES OF LASER ORBITAL TRANSFER VEHICLE

A LOTV vehicle is considered as a space tug-boat for transferring large-size debris objects from LEO to GEO or into a “libration point” in the Earth–Moon system. That is why the vehicle is expected to have a large inertial mass about 10 t. To provide a continuous mode of the thrust production independently of atmosphere conditions, an air-born laser with a power of 500 kW is assumed to be used (Fig. 2) [6]. In this case, the produced thrust of 100 N is much less than the gravitational forces pressing to the vehicle by the Earth. In this case one says about a low-thrust maneuver mode of the vehicle mission from orbit to orbit by a spiral trajectory [13], and the orbital transferring time depends on both the vehicle mass and the laser propulsion efficiency.

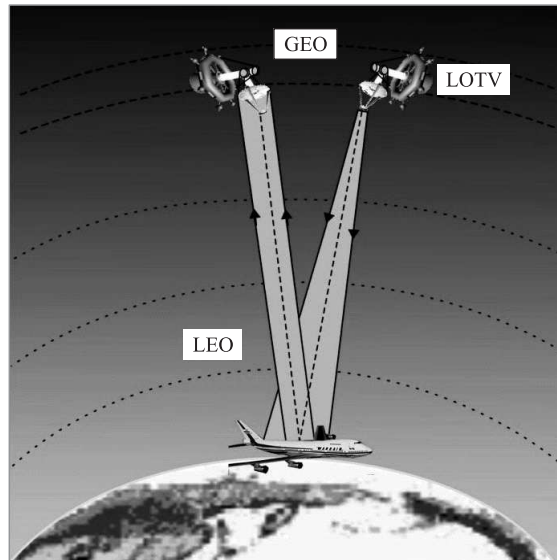


Figure 2 The LOTV (“space tugboat”) concept. LOTV mass $M_0 \approx 10$ t; operating cycle ~ 1 month; and airborne laser power ≈ 500 kW

To define the laser energy consumption for the LOTV orbital mission, such parameter as expenditure of the laser energy C_e [7] was applied to transfer a unit mass (kilogram) of the LOTV payload up to a high orbit. In the analysis, the following conditions of the LOTV mission have been taken into consideration:

- transferring of LOTV is run with a variable vehicle mass;
- specific impulse I_{sp} of LPE is an optimal one satisfying the conditions of high production efficiency of laser propulsion; and
- the energy cost of the orbital LOTV maneuver is a function of both the LOTV receiver aperture and the LPE thrust and specific impulse.

To analyze the space maneuver of LOTV, the transfer scenario of the vehicle within a coplanar trajectory was considered. The vehicle has the initial velocity V_{LEO} and mass M_0 . Moreover, the fact that the LOTV receiver mirror collecting incoming laser beam intercepts only a portion of the laser power because the mirror is limited by its aperture was taken into account. In the diffraction approximation, the portion of the laser power collected by the mirror comes in terms of spherical Bessel function J_0 as follows:

$$\eta_{\text{dif}} = 1 - J_0^2 \left(\frac{\pi}{2} \frac{d_{\text{em}} d_{\text{rec}}}{\lambda(r - R_{\text{Earth}})} \right) - J_1^2 \left(\frac{\pi}{2} \frac{d_{\text{em}} d_{\text{rec}}}{\lambda(r - R_{\text{Earth}})} \right)$$

where R_{Earth} is the Earth radius; d_{em} and d_{rec} are the diameters of the transmitter and receiver mirrors; and r is the current orbit radius. The use of airborne lasers imposes also some limitations on the aperture of the laser transmitter telescope. The transmitter mirror diameter will most likely be not more than 1.5 m.

The total mass of the LOTV is taken to be equal to the sum of the initial mass of the vehicle M_0 and the receiver mirror mass M_{mir} . The initial mass M_0 includes the debris and the propellant masses. The present-day technology used for manufacturing of large-aperture space mirrors gives a distributed mass of the receiver of $1-5 \text{ kg/m}^2$ [14]. That means the mass of a 30-meter receiver can run up to 3 t. This is quite comparable with M_0 (10 t), and it will increase the period of the LOTV space mission and the mission energy expenditure. It is suggested the LPE mass is negligibly small as compared with the LOTV mass. The efficiency of the conversion of the laser power into kinetic power of the exhaust jet η is chosen to be constant and equal to 0.6.

In the LOTV maneuver model, it is assumed that the vehicle has the velocity \vec{V} at start moment and the momentum impulse $\vec{p}_{\text{in}} = (M + \Delta m)\vec{V}$. The propellant consumption mass Δm is ejected at a velocity \vec{V}_E in the vehicle spatial value system. As a result, the total final impulse of the space vehicle and of the propellant mass will be equal to $\vec{p}_{\text{fin}} = M(\vec{V} + \overline{\Delta V}) + \Delta m(\vec{V} + \overline{\Delta V}_E)$

Table 2 The LOTV mission from LEO to a libration point of the Earth–Moon system ($C_m = 12.23 \cdot 10^{-5}$ N/W; thrust = 122.36 N; and propellant consumption = 12.48 g/s)

LOTV initial mass M_0 , t (two versions)	LOTV receiver mirror diameter D , m	Payload mass delivered to a libration point M_{pl} , t	Total mission period, 24 h	Specific energy consumption C_e , MJ/kg
10.39/100.39	10	1.75/32.4	6.3/48.8	309/130
11.57/101.57	20	1.11/31.8	6.9/49.35	535/134
13.534/103.534	30	0.52/30.8	7.84/50.3	1305/141

in a stationary coordinate system, and increment in $\overrightarrow{\Delta p}$ is described by the formula:

$$\overrightarrow{\Delta p} = M \overrightarrow{\Delta V} + \Delta m \vec{V}_E.$$

Taking into account that $\Delta m = -\Delta M$ and using the Newton's second law of motion $d\vec{p}/dt = \vec{F}$, one can get [13]:

$$\frac{d\vec{p}}{dt} = M \frac{d\vec{V}}{dt} - \frac{dM}{dt} \vec{V}_E = -\gamma \frac{M_{\text{Earth}} M}{r^3} \vec{r} \quad (2)$$

or

$$\frac{d\vec{V}}{dt} - \frac{\vec{V}_E}{M} \frac{dM}{dt} = -g \frac{R_{\text{Earth}}^2}{r^3} \vec{r}. \quad (3)$$

The calculations made by using (2) and (3) show that the minimum of the energy expenditure per 1 kg of payload C_e increases with the increase of the specific impulse. And the optimal diameter of the receiver mirror constitutes $D_{\text{LOTV}} \sim 17$ m, C_e comes to $1.6 \cdot 10^8$ J/kg for $\lambda = 1.06 \mu\text{m}$. The estimated receiver diameter is a crucial point in many respects, if the atmosphere effects on the efficiency of the laser power delivery to the vehicle through the upper atmosphere are to be examined. One should be mentioned that the specific energy consumption by using the solid fuel inter-orbital tug IUS (Inertial Upper Stage) comes to $C_e = 5 \cdot 10^7$ J/kg, and it comes to $2 \cdot 10^8$ J/kg for the mission with a liquid fuel rocket of the “Centaurus” type [15]. But the main advantage of the LOTV space maneuver in respect to the vehicles with a conventional chemical thrust is that the LOTV does not bear an energy supply source on a board.

Similar theoretical estimations of the transfer characteristics of the LOTV from the LEO to the Earth–Moon libration point are listed in Table 2. The LOTV vehicle with two different masses $M_0 = 10$ and 100 t are considered assuming different masses of the debris objects which have to be removed from the LEO in the course of one mission.

As one can see, the smaller is the mirror diameter, the larger is the payload mass delivered to a libration point. The last outcome is particularly evident in

the case of the LOTV with a low initial mass. And only 6 days will require to transfer the LOTV to the libration point in this case. Nevertheless, one may note that the debris inertial mass in the LEO can be reduced to 30 t only during one mission if the LOTV has the primary mirror diameter of 30 m and the initial mass of 100 t.

4 LASER PROPULSION ENGINE FOR SPACE MISSIONS AND LASER THRUSTER FOR SATELLITES

The limited receiver aperture of LOTV results both in decreasing of the laser power delivered to the propulsion engine being on high orbits exceeding 5000 km and in decreasing of the thrust produced by LPE as a consequence. The low-thrust mode of the vehicle flight implies a spiral trajectory of the flight when the spiral orbit is close to a circular orbit. It means that the axis of the laser beam coming to the vehicle does not coincide with the vehicle movement vector, and auxiliary optics have to be applied to direct the laser beam into LPE, providing a freedom of the LOTV orbit maneuvers on a mutual orientation of the vehicle and laser.

For that, it is assumed [6] to use an auxiliary space reflector which would direct the laser beam into the engine nozzle. The reflector has to be arranged in the vehicle orbit or near it and should maneuver in the orbit by the same manner as the vehicle. Moreover, a laser beam directed into LPE from the nozzle exhaust side would be distorted by the exhaust jet. And the combination of the optical and gas-dynamic units as a common unit of the engine [6, 8] would result in a degradation of the optical surface of the nozzle under a load of extremely high temperature plasma, plasma electrons, and the ion flux.

To design the LPE for LOTV, a different approach to designing the engine was used. The approach is based on the constructive and functional separation of the engine optical and nozzle units. The conceptual design of Aerospace LPE (ASLPE) [16] is shown in Fig. 3. Each unit can be separately designed to fully meet the specific characteristics of lasers and to provide given thrust characteristics for specific conditions of the ASLPE operation.

Aerospace LPE operates as follows. A beam from a remote laser passes to the optical receiver system (a radiation collector and additional optical elements) arranged on the vehicle board. The receiver system transforms the laser beam and directs it coaxially to the symmetry axis into the LPE beam concentrator.

The laser beam formed by the optical system is transmitted to the first reflector R1, which is made as a cone-shaped figure of rotation with a generatrix being a part of a parabola. The focus of the mirror R1 is a circle (shown in the figure as a dashed ellipse line), which crosses the plane of the figure in the

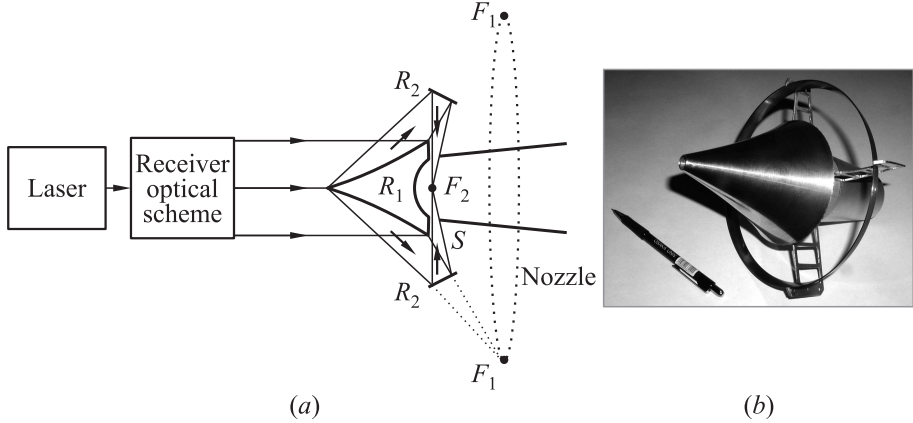


Figure 3 Conceptual design (a) and model photo (b) of ASLPE

point F_1 . The second reflector R_2 changes the position of the beam focus point so that the beam is directed into the nozzle. Generally, the form and sizes of focus region F_2 can change, depending on the shape of generatrix of the reflector R_2 . When the optical parameters of both reflectors are selected, the laser beam is be focused inside the nozzle in such a way that the radiation intensity is great enough to induce a laser breakdown of a solid propellant being arranged closely by the nozzle axis.

The engine nozzle consists of two components — a shock wave impulse receiver and the jet nozzle itself. The pressure impulse receiver and the first reflector are parts of the combined element that is a center-body of the engine. The form and geometry parameters of the pressure impulse receiver are determined at considering an optimum arrangement of the propellant breakdown region about its walls in approach of a theory of local explosion.

There are no optical windows for the radiation input into a nozzle in the ASLPE device. And the gas window can be produced by a boundary of the flow inside the nozzle with an external atmosphere. In this case, an extra external nozzle producing a directed gas flow and an additional thrust is mounted downwards the flow from the engine beam concentrator. Thus, the total effect of two nozzles should result in keeping the specific impulse of the exhaust jet as a whole in a repetitively pulsed mode of laser operation.

The prototype of the aerospace laser propulsion engine (Fig. 3b) was designed and experimentally tested by using a CO₂ laser operating in a repetitively pulsed mode with the pulse energy of 130 J and the pulse repetition rate of 50 Hz, the laser output power was of 6 kW [17]. The total mass of the model is 150 g. Poly-oximethylene (Delrin®) was used as auxiliary propellant to increase a thrust in the experiments. The ASLPE model demonstrated the following laser propulsion characteristics:

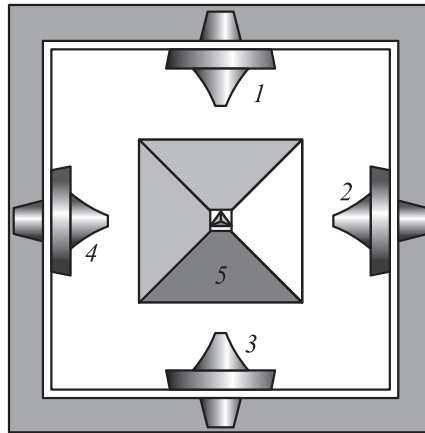


Figure 4 Concept of the laser fine-adjustment thrusters on the base of ASLPE

- momentum coupling coefficient $C_m = 2.5 \cdot 10^{-4}$ N/W; and
- thrust $T = 1.3\text{--}1.5$ N.

Another model of the ASLPE was tested with other CO₂ laser operating in continuous wave (CW) modes. In the experiments, the maximal thrust achieved was 2.0 N under the laser power of 10 kW and at the auxiliary air mass flow of 0.2 g/s. The thrust corresponds to $C_m = 10^{-4}$ N/W.

The suggested device of ASLPE can be easily employed to design a space satellite laser thruster, to arrange on a satellite board till its launching. The thruster is schematically shown in Fig. 4. The thruster combines a four pair wise orthogonal ASLPE (1–4) arranged on an integrated platform. In the center of the platform, a tetrahedral mirror pyramid (5) is installed to direct a laser beam to one (or pair) engines.

A more detailed design of the thruster is shown in Fig. 5 to illustrate how the device can operate. Two possible versions of the propellant storage are shown in the figure. Liquid fuel tanks can be arranged on a platform closely by every engine to inject the fuel into a laser breakdown region of the engine nozzle. Simultaneously, solid propellants can also be installed at the engine axis to decrease the laser intensity threshold initiating the laser ablation process of the propellant.

A reference He–Ne laser is used to stabilize a spatial position of the laser power beam in a plane of the thruster receiver mirror (or rhomb). This operational requirement is caused by the vibration of a satellite construction and by the influence of its motion on the high-power laser radiation delivery to the thruster. To control the optical part of the thruster and operating laser beam,

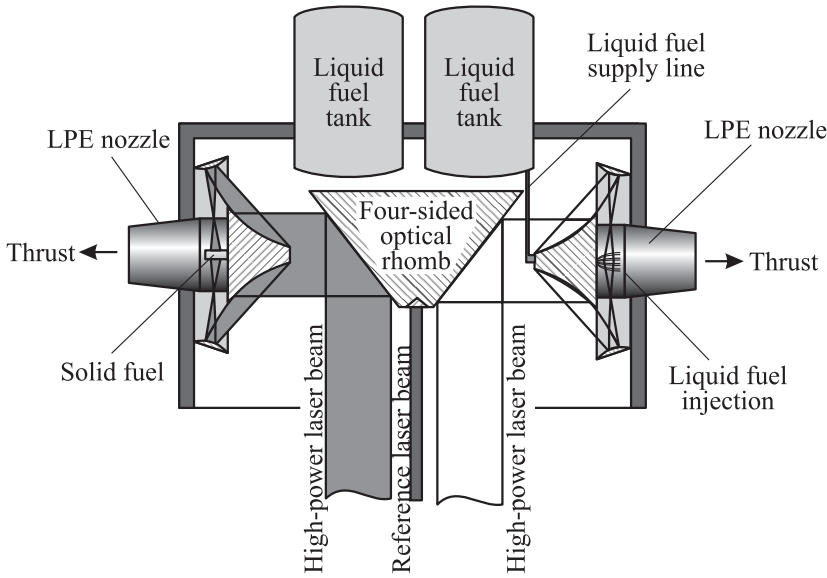


Figure 5 Principal schematic diagram of the laser thruster designed on a basis of ASLPE [18]

the adjustment system is supplied with a laser illumination system by using auxiliary adjusting lasers and retroreflectors arranged on the top of the optical rhomb.

The thruster can be used to control the satellite operational orbit or to remove rocket upper stages back to the Earth. To realize this technique, the thruster has to be arranged onboard of the rocket stage and need only be switched on such a moment of time when the stage moves above a fixed local point of the Earth. The LPE can operate individually or by pairs, producing various directions of the thrust vector depending on the satellite orientation with respect to the orbital motion vector.

The satellite orbit correction or its deorbiting by using the suggested laser thruster can be estimated theoretically by considering the satellite orbital motion as the movement of its center of inertia. In this case, the satellite is considered as a point mass being under the influence of various disturbing forces [18]. The results of the estimations are presented in Table 3, where the following parameters are listed:

- m_{pl}/M is the payload fraction of the total satellite mass after a single orbit adjustment maneuver; and
- C_e is the specific energy consumption of the satellite correction maneuver.

Table 3 Laser thruster characteristics for two cases of the satellite velocity decrement

ΔV , km	η , %	I_{sp} , s	C_m , dyne/W	F_t , N	\dot{m} , g/s	P , kW	m_{pl}/M	Q , kJ/kg	C_e , kJ/kg
20	80	598	217.8	31.8	5.4	14.6	0.993	18,787 (Delrin®)	15.1
	80	1000	364	31.8	3.2	8.76	0.9958	57,000	9.1
100	80	600	219	49.7	8.4	22.7	0.989	18,787 (Delrin®)	22
	80	1000	364	49.7	5.08	13.7	0.994	57,000	13.1

The laser propulsion efficiency is assumed to be maintained at the level of 80% (see Table 1). The first and the second lines represent the laser propulsion characteristics at specified values of the thrust F_t , the combustion energy Q , and the specific impulse I_{sp} .

As is seen, the use of Delrin® (polyoxymethylene) only as a propellant for the laser thruster cannot provide the necessary characteristics of the thrust which are $I_{sp} \sim 1000$ s and $C_m \sim 100$ dyne/W, respectively. To attain these characteristics, a new propellant with the specific combustion heat Q of 57,000 J/kg in the order of magnitude should be created. In this case, the specific energy consumption C_e of the orbit adjustment maneuver, the laser power, and the stored mass of the propellant will be minimal ones.

5 CONCLUDING REMARKS

A laser orbital transfer vehicle as well as a laser thruster can be used to mitigate the problem of space debris accumulation in LEO. An ASLPE operating both in CW and repetitively-pulsed modes is assumed to be used to design a laser propulsion device. To produce a thrust at space conditions efficiently, such power-generating propellant as a polyoxymethylene (Delrin®) is suggested to be used. To increase the propulsion efficiency, a new propellant with a combustion energy of 57,000 kJ/kg should be created.

REFERENCES

1. Phipps, C. R., and M. M. Michaelis. 1994. NEO-LISP: Deflecting near-Earth objects using high average power, repetitively pulsed lasers. *23rd European Conference on Laser Interaction with Matter*. St. John's College, Oxford, England. LA-UR 94-3124.
2. Lobanovsky, Yu. 1996. Concept of an advanced reusable aerospace transportation system. *La Recherché Aerospatiale* 2.

3. Contzen, J. P., and J. Muylaert. 2010. Scientific aspects of space debris re-entry. *ISTC Workshop on Mitigation of Space Debris*. Von Karman Institute for Fluid Dynamics.
4. Launch vehicle energia. http://www.energia.ru/english/energia/launchers/vehicle_energia-pe.html.
5. Kantrowitz, A. 1972. Propulsion to orbit by ground-based lasers. *Aeronautics Astronautics* 10(5):40–42.
6. Nebolsine, P. E., and A. N. Pirri. 2002. Laser propulsion: The early years. *AIP Conference Proceedings* 664:11–21.
7. Rezunkov, Yu. A. 2003. Laser propulsion for LOTV space missions. *AIP Conference Proceedings* 702:228–40.
8. Phipps, C., M. Birkan, W. Bohn, H. Horisawa, T. Lippert, Yu. A. Rezunkov, A. Sasoh, W. Schall, and J. Sinko. 2010. Laser ablation propulsion. *J. Propul. Power* 26(4):609–37.
9. Rezunkov, Yu. A. 2011. Efficiency of high-power laser propulsion. *Int. J. Aerospace Innovations* 3(2):59–75.
10. Ageichik, A. A., E. V. Repina, Yu. A. Rezunkov, and A. L. Safronov. 2009. Detonation of CHO-propellants in a laser propulsion engine. *Russ. J. Techn. Phys.* 54(3):402–9.
11. Assovskiy, I. G. 2005. *Physics of combustion and interior ballistics*. M.: Nauka. 360 p. [In Russian.]
12. Liukonen, R. A. 1992. Efficiency of conversion of radiation power into mechanical pulse in the laser propulsion engine. *Russ. J. Techn. Phys.* 18(7):76–79.
13. Grozdovsky, G. L., Yu. N. Ivanov, and V. V. Tokarev. 1966. *Mechanics of space flights of vehicles with a low thrust*. M.: Nauka.
14. Next generation space telescope. <http://ngst.gsfc.nasa.gov>.
15. Garrison, P., and G. F. Stoky. 1988. Space rocket engines of the future. *J. Propul. Power* 6:520–25.
16. Ageichik, A. A., M. S. Egorov, Yu. A. Rezunkov, A. L. Safronov, and V. V. Stepanov. 2003. Aerospace laser propulsion engine. Russ. Patent No. 2266420.
17. Rezunkov, Yu. A., A. L. Safronov, A. A. Ageichik, and M. E. Egorov. 2005. Performance characteristics of laser propulsion engine operating both in CW and in RP modes. *AIP Conference Proceedings* 830:3–13.
18. Rezunkov, Yu. A., M. S. Egorov, S. G. Rebrov, E. V. Repina, and A. L. Safronov. 2009. Laser fine-adjustment thruster for space vehicles. *AIP Conference Proceedings* 1230:107–17.